Virus Research 273 (2019) 197742

Contents lists available at ScienceDirect

Virus Research

journal homepage: www.elsevier.com/locate/virusres

Characterization of a novel rhabdovirus isolated from a stranded harbour porpoise (*Phocoena phocoena*)

Alexandra Emelianchik[a], Thaís C.S. Rodrigues[a], Kuttichantran Subramaniam[a], Ole Nielsen[b], Kathy A. Burek-Huntington[c], David Rotstein[d], Vsevolod L. Popov[e], David Stone[f], Thomas B. Waltzek[a,*]

[a] University of Florida, 2187 Mowry Road, 32611, Gainesville, Florida, USA
[b] Department of Fisheries & Oceans Canada, 501 University Crescent, Winnipeg, Manitoba, Canada
[c] Alaska Veterinary Pathology Services, 23834 The Clearing Dr, 99577, Eagle River, Alaska, USA
[d] Marine Mammal Pathology Services, 19117 Bloomfield Road, 20832, Olney, Maryland, USA
[e] Department of Pathology, University of Texas Medical Branch, 301 University Boulevard, 77555-0609, Galveston, Texas, USA
[f] Centre for Environment, Fisheries and Aquaculture Science (CEFAS), Weymouth, DT4 8UB, UK

ARTICLE INFO

Keywords:
Rhabdoviridae
Cetacean
Harbour porpoise
Marine mammal

ABSTRACT

An adult male harbour porpoise (*Phocoena phocoena*) stranded off the coast of Alaska displaying poor body condition, scattered mild ulcerative dermatitis, and necrotizing balanoposthitis. Necropsy findings included severe verminous panniculitis, pneumonia, hepatitis, and enteritis. Histopathological examination of skin lesions revealed a pustular epidermitis and dermatitis, with ballooning degeneration of keratinocytes and occasional amphophilic intracytoplasmic inclusion bodies. A swab sample collected from the ulcerative penile lesions was processed for virus isolation resulting in cytopathic effects observed in primary beluga whale kidney (BWK) cells. Transmission electron microscopy revealed bullet-shaped virions budding from the cell surface of infected BWK cells consistent with a rhabdovirus. A cDNA library was prepared using RNA extracted from infected cell culture supernatant and sequenced on an Illumina MiSeq sequencer. The near-complete genome of a novel rhabdovirus was recovered. Genetic and phylogenetic analyses based on the complete L gene supported the harbour porpoise rhabdovirus (HPRV) as a new species. HPRV clustered phylogenetically with dolphin rhabdovirus (DRV) and this cetacean rhabdovirus clade was found to be the sister group to members of the genus *Perhabdovirus* that infect fish. A specific nested RT-PCR assay detected HPRV RNA in the epaxial musculature of the harbour porpoise. Our results are consistent with a previous hypothesis that cetacean rhabdoviruses may have arisen following a host jump from fish and suggest that DRV and HPRV represent separate species belonging in a new genus within the family *Rhabdoviridae*. Further research is needed to determine the health impact of HPRV in harbour porpoise populations, its prevalence, and route of transmission.

1. Introduction

Harbour porpoises (*Phocoena phocoena*) are small odontocetes that belong to the family *Phocoenidae* (Klinowska, 1991; Rice, 1998). They reach up to 2.5 m in total length, weigh up to 115 kg, and are typically observed in groups of 3–5 individuals (Leatherwood et al., 1982). The species occurs along northern temperate subarctic coastlines and due to their wide distribution, synoptic surveys have not been conducted (Hammond et al., 2008). The global abundance of harbour porpoises is estimated to be >700,000 individuals (Hammond et al., 2008) and although the health of these populations are unknown, declines have been reported (Osmek et al., 1996; Reeves and Notarbartolo, 2006). Although considered a species of least concern by the International Union for Conservation of Nature, harbour porpoises are prone to entanglement in fishing gear, preyed on by sharks and killer whales (*Orcinus orca*), and hunted as a food source by native communities in the Northern Hemisphere (Hammond et al., 2008). In addition to anthropogenic threats and predation, these animals are also affected by infectious diseases such as brucellosis resulting in reproductive disease (Dagleish et al., 2008), verminous pneumonia (Jauniaux et al., 2010), and systemic mycosis (Wünschmann et al., 1999).

Harbour porpoises are also known to be infected by both RNA and

* Corresponding author at: Department of Infectious Diseases and Immunology, College of Veterinary Medicine, University of Florida, 2187 Mowry Road, 32611, Gainesville, Florida, USA.
E-mail address: tbwaltzek@ufl.edu (T.B. Waltzek).

https://doi.org/10.1016/j.virusres.2019.197742
Received 10 July 2019; Received in revised form 5 September 2019; Accepted 6 September 2019
Available online 06 September 2019
0168-1702/

DNA viruses. Herpesviruses are double-stranded DNA (dsDNA) viruses that can cause mucocutaneous and systemic diseases in cetaceans including harbour porpoises (Kennedy et al., 1992; Van Elk et al., 2016). Other dsDNA viruses, such as papillomaviruses, have been detected by immunohistochemistry in the cutaneous warts of a harbour porpoise (Van Bressem et al., 1999a). A novel adenovirus was identified in the intestinal contents of harbour porpoises stranded along the Dutch coastline, but typical microscopic lesions induced by adenoviruses were not observed (Van Beurden et al., 2017). A positive-sense single-stranded RNA (ssRNA) virus, determined to be a novel norovirus, was associated with gastroenteritis in a stranded harbour porpoise in the North Sea (De Graaf et al., 2017). Porpoise morbillivirus, a negative-sense ssRNA virus, has resulted in significant harbour porpoise mortality events in the North Sea (Van Bressem et al., 1999b). A rhabdovirus was isolated from a white-beaked dolphin (*Lagenorhynchus albirostris*) that stranded off the coast of the Netherlands in 1992 (Osterhaus et al., 1993). Phylogenetic analysis based on the L gene revealed this virus was a novel rhabdovirus, which was later named dolphin rhabdovirus (DRV) (Osterhaus et al., 1993; Siegers et al., 2014). Serological evidence of DRV in a range of of marine mammals including polar bears, pinnipeds, and cetaceans such as harbour porpoises suggest that exposure to DRV, and perhaps realated rhabdoviruses, may be common in marine mammals (Osterhaus et al., 1993; Philippa et al., 2004; Siegers et al., 2014).

The family *Rhabdoviridae* includes negative-sense ssRNA viruses that are ecologically diverse with 20 genera and >130 known species infecting plants, arthropods, and vertebrates including fish, reptiles, birds, and mammals (Walker et al., 2015; Amarasinghe et al., 2017; Dietzgen et al., 2017; ICTV, 2018; Walker et al., 2018). Rhabdoviruses are responsible for noteworthy diseases in human and veterinary medicine including zoonotic agents transmitted by wildlife such as rabies virus. Herein, we report the virion ultrastructure and genome sequencing of a novel rhabdovirus isolated from a stranded harbour porpoise.

2. Materials and methods

2.1. Sample collection

An adult male harbour porpoise was found stranded alive on September 2013 at Knik Arm, Birchwood, Chugiak, Alaska. Two days later the animal was examined and euthanized after it was determined to be severely debilitated. The carcass was necropsied under the Marine Mammal Health and Stranding Reponses Program permit 932-1905-00/MA-009526. Tissue samples were collected, fixed in 10% neutral buffered formalin, and routinely processed for histopathological analysis. Additional samples of liver, kidney, spleen, testicle, heart, and epaxial muscle where frozen at −80 °C. Tissue samples from skin lesions were collected in viral transport medium (VTM) and subjected to PCR assays for herpesvirus and morbillivirus identification at the Athens Veterinary Diagnostic Laboratory, using previously described methodologies (VanDeVanter et al., 1996; Tong et al., 2008). Swabs from penile lesions were collected in VTM and stored at −80 °C for virus isolation.

2.2. Virus isolation

Swab samples were processed for routine virus isolation (Chan and Hsiung, 1994) using primary beluga whale (*Delphinapterus leucas*) kidney (BWK) cells (Nielsen et al., 1989). Frozen ampoules containing swab samples were rapidly thawed and aliquots of 350 µl were aseptically inoculated onto 70% confluent 25 cm^2 tissue culture flasks (Corning Inc., Corning, NY, USA). A mock-infected flask inoculated with sterile media served as negative control. Inoculum was allowed to adsorb for an hour at 37 °C before being replaced with 5 ml of cell culture medium Dulbecco's Minimal Essential Medium/Ham's F-12 (1:1) (HyClone Inc., Logan, UT, USA), containing antibiotics (penicillin 200 IU/ml, streptomycin 200 µg/ml and gentamycin 50 µg/ml) and 10% fetal bovine serum, as previously described (Tuomi et al., 2014). Flasks were incubated at 37 °C and observed daily for the presence of cytopathic effects (CPE) using an inverted microscope. Flasks were sub cultured (1:2) into fresh media weekly for four weeks before discarding. Media from flasks showing CPE was passed through a 0.45 µm filter, diluted (1/100) and passaged onto fresh cells. When CPE could be successfully passaged, the presumptive virus isolate was included for further study.

2.3. Transmission electron microscopy

The supernatant of a 75 cm^2 flask of infected BWK cells displaying extensive CPE was discarded and the monolayer was fixed in 15 ml of modified Karnovsky's fixative (2P + 2 G, 2% formaldehyde prepared from paraformaldehyde and 2% glutaraldehyde in 0.1 M cacodylate buffer pH 7.4) for 2 h at room temperature. The monolayer was washed in cacodylate buffer, scraped off the flask and pelleted. The pellet was shipped in PBS overnight on ice packs to the University of Texas Medical Branch Department of Pathology Electron Microscopy Laboratory (UTMB-EML). At UTMB-EML, the cell pellet was washed in cacodylate buffer and left in 2P + 2 G fixative overnight at 4 °C. The next day the cell pellet was washed twice in cacodylate buffer, post-fixed in 1% OsO4 in 0.1 M cacodylate buffer pH 7.4, *en bloc* stained with 2% aqueous uranyl acetate, dehydrated in ascending concentrations of ethanol, processed through propylene oxide and embedded in Poly/Bed 812 epoxy plastic (Polysciences, Warrington, PA, USA). Ultrathin sections were cut on a LEICA EM UC7 ultramicrotome (Leica Microsystems, Buffalo Grove, IL, USA), stained with 0.4% lead citrate, and examined in a JEM-1400 electron microscope (JEOL USA, Peabody, MA, USA) at 80 kV.

2.4. Genome sequencing

RNA was extracted from BWK cell culture supernatant using a QIAamp Viral RNA Mini Kit (Qiagen, Valencia, CA, USA) according to the manufacturer's recommendation. A cDNA library was generated using a NEBNext Ultra RNA Library Prep Kit (Illumina, San Diego, CA, USA) and sequenced on an Illumina MiSeq sequencer. *De novo* assembly of 2,607,928 paired-end reads was performed using SPAdes 3.5.0 (Bankevich et al., 2012). The resulting contigs were subjected to BLASTX searches against a proprietary viral database created in CLC Genomics Workbench 10.1.1 from virus protein sequences retrieved from the UniProt Knowledgebase (https://www.uniprot.org/uniprot/). The quality of the assembly was evaluated by mapping the reads back to the consensus sequence in Bowtie 2.1.0 (Langmead and Salzberg, 2012) and then the alignment was visualized in Tablet 1.14.10.20 (Milne et al., 2010). Putative open reading frames (ORFs) were predicted using GeneMarkS (http://exon.biology.gatech.edu/) (Besemer et al., 2001) and gene function was predicted using BLASTP searches against the National Center for Biotechnology Information (NCBI) GenBank non-redundant protein sequence database.

2.5. Phylogenetic and genetic analyses

The complete L gene amino acid (aa) sequences for 48 rhabdoviruses were retrieved from the NCBI GenBank database (Table 1) and aligned to the sequence generated in this study using Multiple Alignment using Fast Fourier Transform 7.0 (MAFFT) software with default parameters. Poorly aligned regions were trimmed from the multiple sequence alignment using the Gblocks Server (http://molevol.cmima.csic.es/castresana/Gblocks_

server.html), with default settings. A Maximum Likelihood phylogenetic tree was generated in IQ-TREE (http://iqtree.cibiv.univie.ac.at/) with the Bayesian information criterion to determine the best model fit and 1000 non-parametric bootstraps to test clade robustness

Table 1
Virus species, virus name, and GenBank sequence accession numbers of 48 rhabdoviruses included in the genetic and phylogenetic analyses.

Virus species	Virus name	GenBank #
—	harbour porpoise rhabdovirus[a]	MN103537
—	dolphin rhabdovirus[a]	YP_009094476.1
—	hybrid snakehead virus[a]	AGI97138
—	Siniperca chuatsi rhabdovirus[a]	ABG76848
—	eelpout rhabdovirus[a]	ALJ30354
—	Scophthalmus maximus rhabdovirus[a]	ADU05406
Alfalfa dwarf cytorhabdovirus	alfalfa dwarf virus	YP_009177021.1
Anguillid perhadbovirus	eel virus European X[a]	AFJ94641
Arboretum almendravirus	Arboretum virus	YP_009094383.1
Bovine fever ephemerovirus	bovine ephemeral fever virus	NP_065409.1
Caligus caligrhavirus	Caligus rogercresseyi rhabdovirus	APF32078
Carp sprivivirus	spring viremia of carp virus	NP_116748.1
Chaco sripuvirus	Chaco virus	YP_009362274.1
Cocal vesiculovirus	Cocal virus	YP_009177651.1
Coffee ringspot dichorhavirus	coffee ringspot virus	AHH44830.1
Curionopolis curiovirus	Curionopolis virus	YP_009094109.1
Drosophila immigrans sigmavirus	Drosophila immigrans sigmavirus	APG78762.1
Drosophila melanogaster sigmavirus	Drosophila melanogaster sigmavirus	ACU65438.1
Durham tupavirus	Durham virus	ADB88761.1
Flanders hapavirus	Flanders virus	AFS68381.1
Fukuoka ledantevirus	Fukuoka virus	YP_009362003.1
Gray Lodge hapavirus	Gray Lodge virus	YP_009362209.1
Hirame novirhabdovirus	hirame rhabdovirus	NP_919035.1
Indiana vesiculovrius	vesicular stomatitis Indiana virus	AMK37545
Itacaiunas curiovirus	Itacaiunas virus	YP_009362166.1
Jurona vesiculovirus	Jurona virus	YP_009094377.1
Klamath tupavirus	Klamath virus	YP_009362266.1
Koolpinyah ephemerovirus	Koolpinyah virus	YP_009177203.1
Lagos bat lyssavirus	Lagos bat virus	YP_007641391.1
Le Dantec ledantevirus	Le Dantec virus	YP_009361873.1
Lepeophtheirus caligrhavirus	Lepeophtheirus salmonis rhabdovirus	AIY25916
Lettuce big-vein associated varicosavirus	lettuce big-vein associated virus	YP_002308576.1
Lettuce necrotic yellows cytorhabdovirus	lettuce necrotic yellows virus	YP_425092.1
Maize mosaic nucleorhabdovirus	maize mosaic virus	YP_052855.1
Moussa virus	Moussa virus	YP009094143
Niakha sripuvirus	Niakha virus	YP_009094471.1
Orchid fleck dichorhavirus	orchid fleck virus	YP_001294929.1
Perch perhabdovirus	perch rhabdovirus[a]	YP_007641367.1
Piscine novirhabdovirus	viral hemorrhagic septicemia virus	CAB44726
Pike fry sprivivirus	pike fry rhabdovirus	YP_009094125.1
Potato yellow dwarf nucleorhabdovirus	potato yellow dwarf virus	YP_004927971.1
Puerto Almendras almendravirus	Puerto Almendras virus	YP_009094394.1
Rabies lyssavirus	rabies virus	NP_056797.1
Salmonid novirhabdovirus	infectious hematopoietic necrosis virus	AAC42155
Snakehead novirhabdovirus	snakehead rhabdovirus	NP_050585.1
Sweetwater Branch tibrovirus	Sweetwater Branch virus	YP_009362251.1
Tibrogargan tibrovirus	Tibrogargan virus	AJG05826
Xingshan alphanemrhavirus	Xingshan nematode virus 4	APG78847
Xinzhou alphanemrhavirus	Xinzhou nematode virus 4	APG78857

[a] Viruses included in the genetic analyses based on complete/near-complete genome sequences.

(Nguyen et al., 2015). A genetic analysis based on the same L gene amino acid sequences was conducted using the Sequence Demarcation Toolv.1.2 (Muhire et al., 2014) with the MAFFT alignment option implemented. Additional genetic analyses were performed using the nucleotide sequences of the L gene or complete/near-complete genome sequences for eight of the aforementioned 48 rhabdoviruses (Table 1).

Table 2
Primers designed for screening harbour porpoise tissue samples for the harbour porpoise rhabdovirus (HPRV) by nested reverse transcription PCR.

Primer name	Sequence
HPRV-F1	GGGTAAAACAAATGGCCCGA
HPRV-R1	TCCGGAGTTCTCAGCATCTC
HPRV-F2	GGCAACTTAGCCAAACTGGT
HPRV-R2	CCCTGGCATATTTGGTTCTG

2.6. Development of a HPRV nested RT-PCR assay

A specific nested endpoint reverse transcription PCR (RT-PCR) assay was designed to amplify a 577 bp region of the HPRV L gene on the first round of amplification and 328 bp on the second round of amplification (Table 2). The nested RT-PCR assay was used to screen liver, kidney, spleen, testicle, heart, and epaxial muscle tissues. RNA from the tissue samples was extracted using a QIAamp Viral RNA Mini Kit according to the manufacturer's recommendation. The first round of the assay was performed using a Qiagen OneStep RT-PCR Kit with 30 µL cocktails consisting of 1.2 µL Enzyme Mix, 6 µL 5X RT-PCR buffer, 6 µL 5x Q-solution, 1.2 µL 10 mM dNTP Mix, 1.2 µL 20 µM forward and reverse primers, 8.4 µL RNase-free water, and 4.8 µL extracted RNA. The RNA extracted from the supernatant of a BWK cell culture displaying CPE was used as a positive control and RNase-free water was used as a negative control. The following steps were used for the first round of amplification: one cycle of 50 °C for 30 min for cDNA synthesis and one cycle of 95 °C for 15 min for denaturing, followed by 40 cycles of denaturation at 95 °C, annealing at 56 °C (primers HPRV-F1, HPRV-R1), and elongation at 72 °C for 30 s each, and a final elongation step at 72 °C for 10 min.

The second round of the assay was performed uisng an Invitrogen Platinum Taq DNA Polymerase Kit with 30 µl conventional PCR cocktails consisting of 17.55 µL molecular grade water, 3 µL 10 × PCR buffer, 1.2 µL 50 mM $MgCl_2$, 0.6 µL 10 mM dNTPs, 1.5 µL 20 mM forward (HPRV-F2) and reverse primers (HPRV-R2), 0.15 µl Taq DNA polymerase, and 4.5 µL of the first round product. The following steps were used for the second round of amplification: an initial denaturation step of 95 °C for 5 min was followed by 40 cycles of a 95 °C denaturation step, a 48 °C annealing step, and a 72 °C extension step, each run for 1 min, and a final extension step at 72 °C for 10 min. The PCR product from the second round was subjected to electrophoresis on a 1% agarose gel stained with ethidium bromide. Bands of the expected size (i.e., 328 bp) were extracted and purified using a QIAquick PCR Purification Kit and sequenced in both directions on an automated ABI 3130 DNA sequencer (Life Technologies, Carlsbad, CA).

3. Results

3.1. Gross and microscopic pathology

Necropsy revealed systemic disease as evident from the observed poor body condition, degenerative myopathy of the sternohyoideus muscle, and severe parasitism of subcutaneous, biliary, hepatic, pulmonary, and gastrointestinal tissues. The mediastinal and prescapular lymph nodes were enlarged and edematous. The animal presented with a mild ulcerative dermatitis characterized by fine ulcers scattered across the body and larger (0.5 cm diameter) ulcers along the abdomen. There was severe multifocal necrotizing balanoposthitis characterized by fibrinopurulent discharge from the prepucial opening and several distinct, sharply defined black ulcers along the shaft and base of the penis, often covered by fibrinopurulent exudate (Fig. 1A and B). Microscopically, ulcers and erosions with underlying hemorrhage were

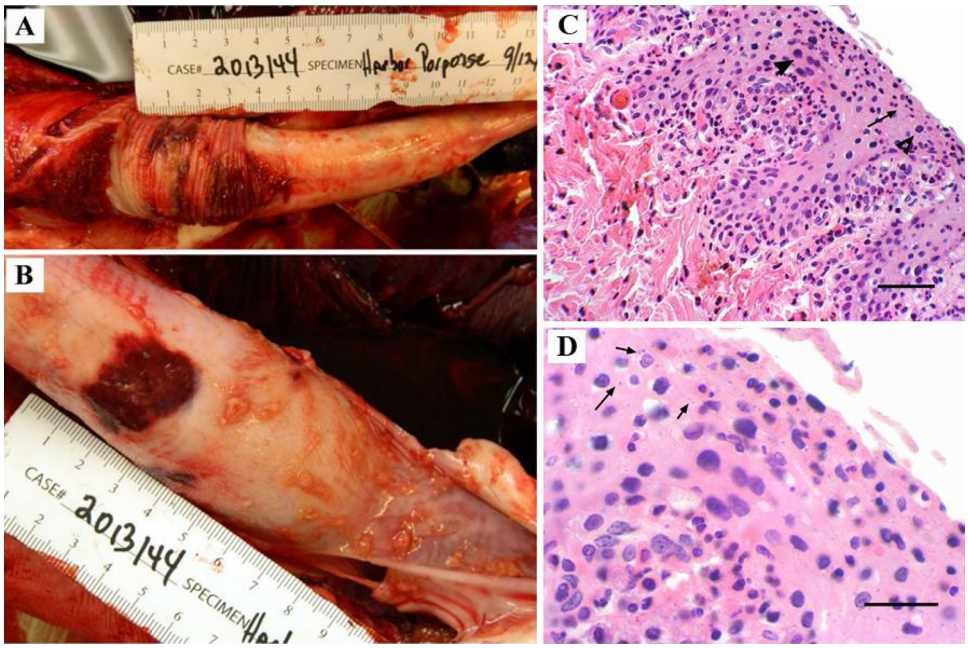

Fig. 1. Gross (A and B) and microscopic (C and D) lesions associated with necrotizing balanoposthitis in an adult harbour porpoise (*Phocoena phocoena*). (A) Ulcers on the prepuce and base of the penis covered in a fibrinopurulent exudate. (B) Sharply defined black ulcer at the base of the penis. (C) Penile epithelium adjacent to the ulcers heavily infiltrated by neutrophils and macrophages (arrow), epithelial cells presenting with swollen nuclei, flat chromatin (arrowhead; Scale bar = 40 μm), (D) and fine intracytoplasmic amphophilic inclusion bodies (arrows; Scale bar = 20 μm).

observed in the preputial and penile epithelia. The epithelium adjacent to the ulcer was heavily infiltrated by neutrophils and macrophages (Fig. 1C). Epithelial cells often demonstrated swollen nuclei with flat chromatin and fine intracytoplasmic amphophilic inclusion bodies (Fig. 1D). The stroma was infiltrated by mixed inflammatory cells including lymphocytes, plasma cells, neutrophils, and macrophages.

Endoparasitism of the lung, liver, and intestine was observed with varying intensities of inflammatory responses. In the lung, there was a moderate eosinophilic and histiocytic bronchopneumonia with numerous adult and larval nematodes present. In the liver, proliferative cholangitis and biliary hyperplasia and trematodes within distended bile ducts were observed. Nematode ova and trematodes were present in the intestines. Mesenteric lymph nodes were hyperplastic with increased eosinophils and few granulomas with rare nematode larvae. Brain and spinal cord sections showed moderate congestion with occasional perivascular hemorrhage.

3.2. Virus isolation and transmission electron microscopy

The inoculated BWK flasks showed evidence of generalized CPE such as enlargement, rounding, and refractility 12 days post infection (DPI) (Fig. 2A and B). Some cells became increasingly refractile in appearance and the cells started to detach from the cell sheet after an additional 24 to 48 h. Ultrastructural examination revealed enveloped virions with bullet-shaped nucleocapsids budding from the surface of the BWK cells (Fig. 2C and D). The mean width and length of the virions were approximately 73 nm (n = 17) and 111 nm (n = 17), respectively.

3.3. Genome sequencing, phylogenetic, and genetic analyses

The *de novo* assembly produced a contiguous consensus sequence of 10,988 bp with a G + C content of 39.87%. The terminal leader and trailer sequences could not be determined. The genome sequence of the harbour porpoise rhabdovirus (HPRV) has been deposited under the NCBI GenBank accession number MN103537. A total of 222,189 reads (8.52%) aligned at an average coverage of 3917 reads/nucleotide. Five ORFs were predicted encoding the nucleoprotein (N), phosphoprotein (P), matrix protein (M), glycoprotein (G), and RNA-dependent RNA polymerase (L; RdRp) (Supplementary Table 1). The genes in the HPRV genome were separated by intergenic regions (Fig. 3A) and six conserved motifs were observed in the RdRp including GHP, premotif A, motif A, B, C, and D in the central region (Fig. 3B).

The best-fit model for the ML analysis based on the aligned L gene sequences was determined to be LG with a four-category gamma distribution of rate variation (LG + G4). HPRV formed a well-supported clade with DRV and the cetacean rhabdovirus clade was found to be the sister group to members of the genus *Perhabdovirus* (Fig. 4). Scophthalmus maximus rhabdovirus branched as the closest relative to the clade composed of the cetacean rhabdoviruses and perhabdoviruses.

Genetic analysis of the HPRV L gene displayed between 23.1–68.3% aa identity to other rhabdoviruses with highest identity to DRV (Supplementary Fig. 1). HPRV shared 65.7% nucleotide identity to DRV and 59.2% nucleotide identity (55.5% aa identity) to the perch rhabdovirus (PRV) in the L gene (Supplementary Figs. 1 and 2). The HPRV and DRV genomes displayed 62.5% nucleotide sequence identity to each other and 53.5–57.9% nucleotide sequence identity when compared to perhabdoviruses and Scophthalmus maximus rhabdovirus (Supplementary Fig. 2).

3.4. Diagnostic PCR assays

The skin lesion samples tested negative for morbillivirus and herpesvirus by PCR. Liver, kidney, spleen, testicle, and heart tissue samples were negative by the HPRV nested RT-PCR assay designed in this study, while the sample from epaxial muscle was positive. The purified RT-PCR product was submitted for Sanger sequencing and confirmed to be identical to the near-complete genome sequence assembled from the Illumina MiSeq data.

4. Discussion

In this investigation, we report the near-complete genome sequence of a rhabdovirus isolated from a stranded harbour porpoise (*Phocoena phocoena*) in Alaska. The *in vitro* growth conditions, virion ultrastructure, and genetic/phylogenetic analyses supported the harbour porpoise rhabdovirus (HPRV) as a novel rhabdovirus most closely related to the DRV (Siegers et al., 2014). To the authors' knowledge, HPRV is the first rhabdovirus isolated and its genome sequenced from a harbour porpoise and only the second rhabdovirus characterized from a cetacean.

The only other known cetacean rhabdovirus, DRV, was isolated in 1992 from the lungs and kidneys of a white-beaked dolphin that

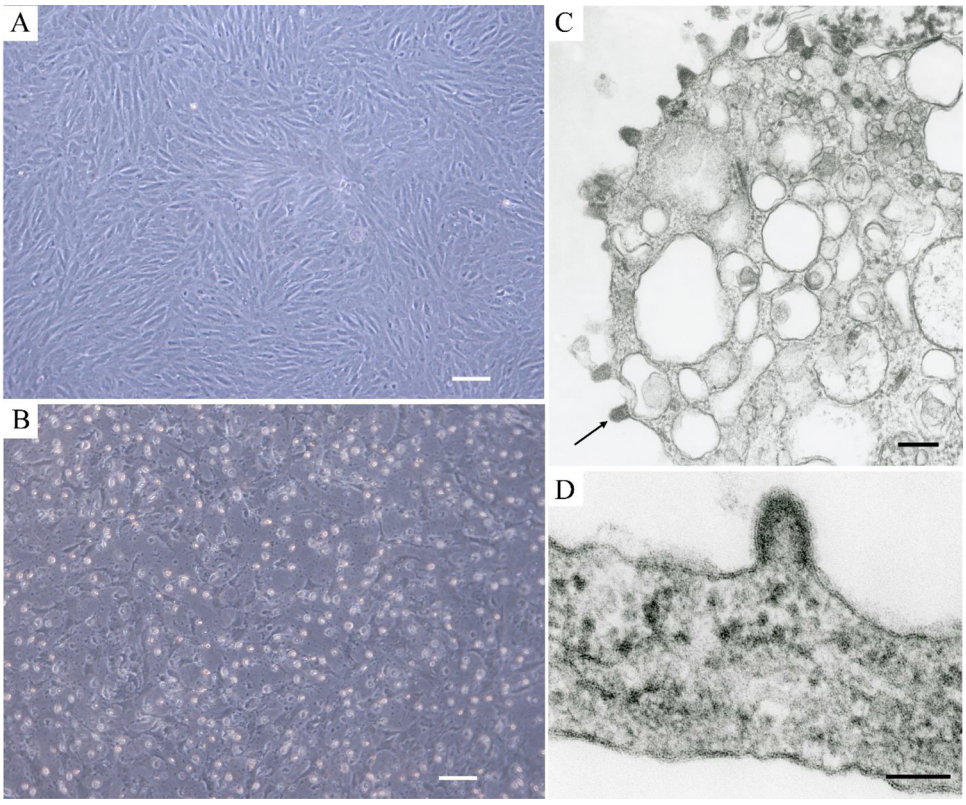

Fig. 2. Cell culture (A and B) and transmission electron photomicrographs of primary beluga whale kidney (BWK) cells infected with harbour porpoise rhabdovirus (C and D). (A) Uninfected BWK cells. Scale bar = 100 µm. (B) Infected BWK cells 9 days post-infection showing rounded, enlarged, and refractile cells. Scale bar = 100 µm. (C) Multiple enveloped viral particles with bullet-shaped nucleocapsids budding from the BWK cell membrane (arrow). Scale bar = 200 nm. (D) Higher magnification of the bullet-shaped virus particle budding from the BWK cell membrane. Scale bar = 100 nm.

stranded on the Dutch coast (Osterhaus et al., 1993). The DRV genome sequence was determined in 2014 and argued to represent a novel cetacean rhabdovirus species (Siegers et al., 2014). Since its discovery, a range of marine mammals including polar bears, pinnipeds, and cetaceans such as harbour porpoises have been shown to carry neutralizing anti-DRV antibodies (Osterhaus et al., 1993; Philippa et al., 2004; Siegers et al., 2014). These serological findings suggest that exposure to DRV, and perhaps related rhabdoviruses such as HPRV, may

A

Gene junction	Polyadenylation signal	Intergenic sequence	Transcription start site
3'/N			UUG
N/P	AUACUUUUUUU	GGAG	UUG
P/M	AUACUUUUUUU	CA	UUG
M/G	AUACUUUUUUU	AG	UUG
G/L	AUACUUUUUUU	GA	UUG
L/5'	AUACUUUUUUU		

B

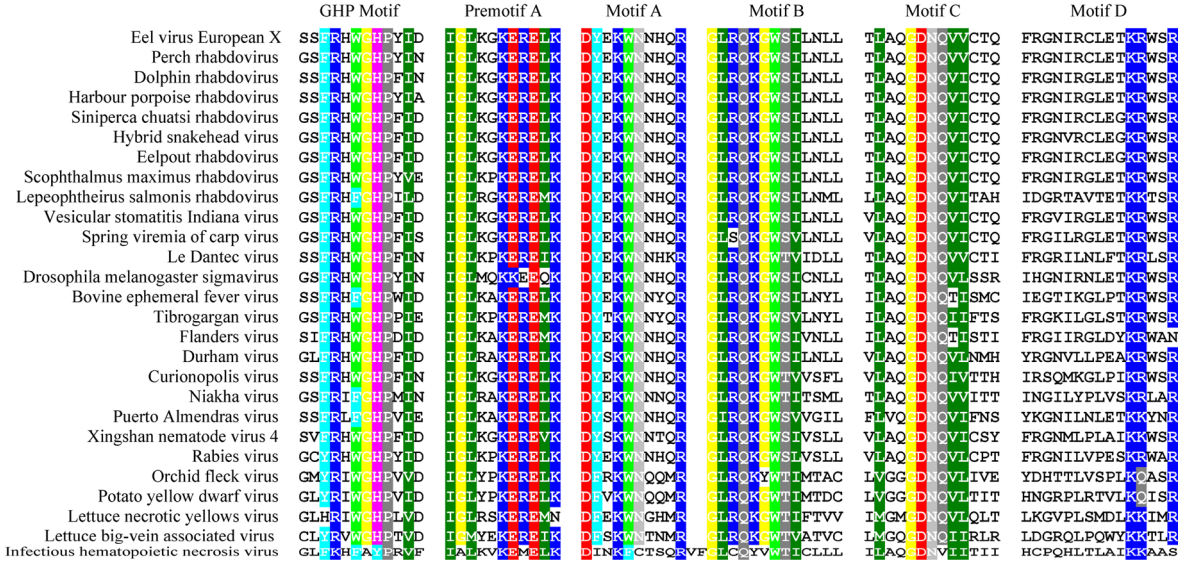

Fig. 3. Genomic characterization of the harbour porpoise rhabdovirus. (A) The intergenic regions of the HPRV genome. (B) Amino acid (aa) sequence alignment displaying conserved domains of the HPRV L gene (RNA-dependent RNA polymerase) when compared to other rhabdoviruses.

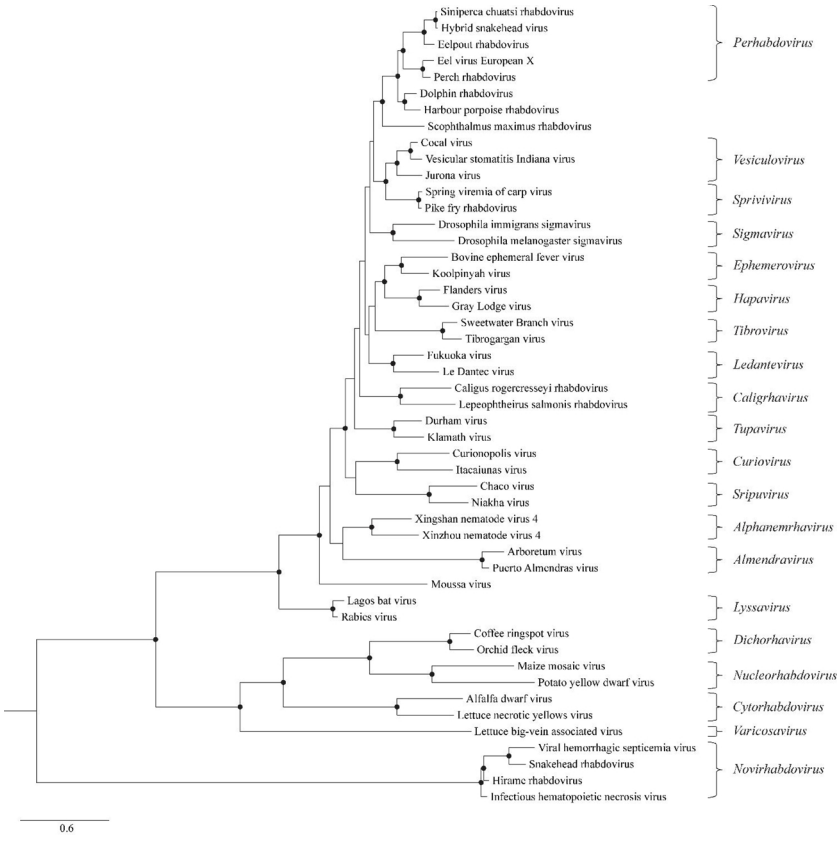

Fig. 4. Maximum Likelihood phylogram depicting the relationship of the harbour porpoise rhabdovirus to 48 other members of the family *Rhabdoviridae* based on the amino acid sequence alignment of the complete L gene. Virus names are listed at the tips of the tree and those assigned to a genus are indicated by brackets to the right of the tree. Nodes with bootstrap values >75% are indicated by black circles and branch lengths are based on the number of inferred substitutions as indicated by the scale.

be common in marine mammals (Osterhaus et al., 1993).

Similar to DRV, the HPRV genome possesses the expected characteristics of a rhabdovirus, including genome length (ranging between 10,000–16,000 bp) and organization (encoding N, P, M, G and L proteins) (Walker et al., 2015, 2018). Ultrastructural examination of HPRV-infected BWK cells revealed virions of the size and shape expected for vertebrate-infecting rhabdoviruses (Hummeler et al., 1967; Dietzgen et al., 2017; Walker et al., 2018). HRPV and its closest relative DRV formed a well supported clade separated from known genera in the family *Rhabdoviridae*. According to the International Committee on Taxonomy of Viruses (ICTV), rhabdoviruses are assigned to genera based on Maximum Likelihood analysis of the L gene (Walker et al., 2018). Demarcation of different genera and species in the family *Rhabdoviridae* varies considerably. For example, the genetic distance between spring viremia of carp virus and vesicular stomatitis Indiana virus, assigned as the type species of the genera *Sprivivirus* and *Vesiculovirus*, based on the complete L protein sequence is similar to the distance between two species (koolpinyah virus and bovine ephemeral virus) currently assigned to the genus *Ephemerovirus*. However, genetic distance is only one criterion that can be used when attempting to demarcate genera and significant differences in genome architecture, antigenicity, and ecological properties such as host range can be important and often useful features when trying to resolve such issues (Walker et al., 2018).

The cetacean rhabdovirus clade is the sister group to the genus *Perhabdovirus* which includes viruses that infect teleost fish (Walker et al., 2018). Similar to the other fish rhabdoviruses from the genus *Sprivivirus,* replication range of perhabdoviruses is lower than those of the mammalian rhabdoviruses, reflecting the aquatic poikilothermic nature of the host species, and the perhabdoviruses are typically isolated in cultured fish cell lines at 15–25 °C. In the case of DRV and HPRV, the viruses have a mammalian host and replicate at 37 °C temperature in mammalian cells (Siegers et al., 2014). This, together with the genetic distance of 55.5–56.1% in the aa sequences of the L gene compared to PRV, suggests that DRV and HPRV more likely represent viruses of a novel genus rather than belonging to the genus *Perhabdovirus*. Further, the high degree of aa sequence divergence in the L gene between DRV and HPRV of 31.7%, suggests that they represent separate species within the new genus. A formal proposal will need to be submitted to the ICTV, but we suggest DRV and HPRV could be considered representatives of a new genus, cetarhabdovirus, to reflect their isolation from cetaceans, and that DRV and HPRV represent new virus species, Dolphin cetarhabdovirus and Porpoise cetarhabdovirus, to reflect the host species from which they were isolated.

In this study, the HPRV viral load would appear to have been relatively low and suggests that it may be a coincidental finding rather than the primary cause of the harbour porpoise stranding. The initial inoculation on BWK flasks first showed evidence of generalized CPE 12 DPI which would be unexpected if the virus was actively replicating in the host during an acute phase of disease. The nested RT-PCR assay results also suggested a low HPRV viral load since the epaxial muscle sample was the only positive sample after the second round of amplification. Additionally, the epaxial muscle sample displayed no significant microscopic lesions as might have been expected if a significant HPRV infection had occurred in this tissue.

In marine mammals, limited information is available regarding the clinical signs or pathology associated with rhabdovirus infections. Both the white-beaked dolphin, from which DRV was recovered, and the stranded harbour porpoise reported here presented in poor body condition. No information was available on the pathology presented by the white-beaked dolphin, except it died in respiratory distress (*i.e.*, severe dyspnea; Osterhaus et al., 1993). In addition, the harbour porpoise presented with a variety of parasitic lesions in multiple organs in addition to an ulcerative balanoposthitis associated with the isolation of HPRV. Further research is needed to determine the role of cetacean rhabdoviruses in disease, their prevalence, and transmission routes.

Acknowledgements

The authors wish to thank the University of Alaska Museum of the North and Dr. Jerry Saliki of the Athens Veterinary Diagnostic Laboratory for their assistance in obtaining and testing harbour porpoise samples, respectively. The authors also wish to thank Dr. Gael Kurath (US Geological Survey Western Fisheries Research Center and member of the International Committee on Taxonomy of Viruses) for an early critique of the manuscript.

Appendix A. Supplementary data

Supplementary material related to this article can be found, in the online version, at doi:https://doi.org/10.1016/j.virusres.2019.197742.

References

Amarasinghe, G.K., Bào, Y.M., Basler, C.F., Bavari, S., Beer, M., Bejerman, N., et al., 2017. Taxonomy of the order mononegavirales. Arch. Virol. 162, 2493–2504. https://doi.org/10.1007/s00705-017-3311-7.

Bankevich, A., Nurk, S., Antipov, D., Gurevich, A.A., Dvorkin, M., Kulikov, A.S., Lesin, V.M., Nikolenko, S.I., Pham, S., Prjibelski, A.D., Pyshkin, A.V., Sirotkin, A.V., Vyahhi, N., Tesler, G., Alekseyev, M.A., Pevzner, P.A., 2012. SPAdes: a new genome assembly algorithm and its applications to single-cell sequencing. J. Comput. Biol. 19, 455–477. https://doi.org/10.1089/cmb.2012.0021.

Besemer, J., Lomsadze, A., Borodovsky, M., 2001. GeneMarkS: a self-training method for prediction of gene starts in microbial genomes. Implications for finding sequence motifs in regulatory regions. Nucleic Acids Res. 29, 2607–2618.

Chan, V.F., Hsiung, G.D., 1994. Cell culture preparation. In: Hsiung, G.D., Fong, C.K.Y., Landry, M.L. (Eds.), Hsiung'S Diagnostic Virology as Illustrated by Light and Electron Microscopy, 4th ed. Yale University Press, New Haven Connecticut, USA, pp. 337–374.

Dagleish, M.P., Barley, J., Finlayson, J., Reid, R.J., Foster, G., 2008. Brucella ceti associated pathology in the testicle of a harbour porpoise (Phocoena phocoena). J. Comp. Pathol. 139, 54–59. https://doi.org/10.1016/j.jcpa.2008.03.004.

De Graaf, M., Bodewes, R., van Elk, C.E., van de Bildt, M., Getu, S., Aron, G.I., Verjans, G.M., Osterhaus, A., van den Brand, J., Kuiken, T., Koopmans, M., 2017. Norovirus infection in harbour porpoises. Emerg. Infect. Dis. 23, 87–91. https://doi.org/10.3201/eid2301.161081.

Dietzgen, R.G., Kondo, H., Goodin, M.M., Kurath, G., Vasilakis, N., 2017. The family Rhabdoviridae: mono- and bipartite negative-sense RNA viruses with diverse genome organization and common evolutionary origins. Virus Res. 227, 158–170. https://doi.org/10.1016/j.virusres.2016.10.010.

Hammond, P.S., Bearzi, G., Bjørge, A., Forney, K., Karczmarski, L., Kasuya, T., Perrin, W.F., Scott, M.D., Wang, J.Y., Wells, R.S., Wilson, B., 2008. Phocoena phocoena. The IUCN Red List of Threatened Species. IOP Publishing IUCNhttps://doi.org/10.2305/IUCN.UK.2008.RLTS.T17027A6734992.en. Accessed 20 April 2018.

Hummeler, K., Koprowski, H., Wiktor, T.J., 1967. Structure and development of rabies rirus in tissue culture. J. Virol. 1, 152–170.

ICTV, 2018. International committee on taxonomy of viruses. Virus Taxonomy: 2018b Release. EC 50, Washington, DC. accessed on July 26, 2019. http://www.ictvonline.org/virus-Taxonomy.asp.

Jauniaux, T.P., Brenez, C., Fretin, D., Godfroid, J., Haelters, J., Jacques, T., Kerckhof, F., Mast, J., Sarlet, M., Coignoul, F., 2010. *Brucella ceti* infection in harbour porpoise (*Phocoena phocoena*). Emerg. Infect. Dis. 16, 12. https://doi.org/10.3201/eid1612.101008.

Kennedy, S., Lindstedt, I., McAliskey, M., McConnell, S., McCullough, S., 1992. Herpesviral encephalitis in a harbor porpoise (*Phocoena phocoena*). J. Zoo Wildl. Med. 23, 374–379. http://www.jstor.org/stable/20095242.

Klinowska, M., 1991. Dolphins, Porpoises and Whales of the World: The IUCN Red Data Book. IUCN, Gland, Switzerland and Cambridge, U.K, pp. 88–98.

Langmead, B., Salzberg, S.L., 2012. Fast gapped-read alignment with Bowtie 2. Nat. Methods 9, 357–359. https://doi.org/10.1038/nmeth.1923.

Leatherwood, S., Reeves, R., Perrin, W., Evans, W., 1982. Whales, Dolphins and Porpoises of the Eastern North Pacific and Adjacent Arctic Waters: a Guide to the Identification. IOP Publishing Aquatic commons Accessed 20 April 2018. http://aquaticcommons.org/1402/1/NOAA_Tech_Rpt_NMFS_Circular_444.pdf.

Milne, I., Bayer, M., Cardle, L., Shaw, P., Stephen, G., Wright, F., Marshall, D., 2010. Tablet—next generation sequence assembly visualization. Bioinform. 26, 401–402. https://doi.org/10.1093/bioinformatics/btp666.

Muhire, B.M., Varsani, A., Martin, D.P., 2014. SDT: a virus classification tool based on pairwise sequence alignment and identity calculation. PLoS One 9, e108277. https://doi.org/10.1371/journal.pone.0108277.

Nguyen, L.T., Schmidt, H.A., von Haeseler, A., Minh, B.Q., 2015. IQ-TREE: a fast and effective stochastic algorithm for estimating maximum likelihood phylogenies. Mol. Biol. Evol. 32, 268–274. https://doi.org/10.1093/molbev/msu300.

Nielsen, O., Kelly, R.K., Lillie, W.R., Clayton, J.W., Fujioka, R.S., Yoneyama, B.S., 1989. Some properties of a finite cell line from beluga whale (*Delphinapterus leucas*). Can. J. Fish. Aquat. Sci. 46, 1472–1477. https://doi.org/10.1139/f89-188.

Osmek, S., Calambokidis, J., Laake, J., Gearin, P., DeLong, R., Scordino, J., Jeffries, S., Brown, R., 1996. Assessment of the Status of Harbour Porpoises, *Phocoena phocoena*, in Oregon and Washington Waters. US. Dep. IOP Publishing NOAA Accessed 20 April 2018. http://www.nmfs.noaa.gov/pr/sars/2013/po2013_harbourporpoise-norwac.pdf.

Osterhaus, A.D., Broeders, H.W., Teppema, J.S., Kuiken, T., House, J.A., Vos, H.W., 1993. Isolation of a virus with rhabdovirus morphology from a white-beaked dolphin (*Lagenorhynchus albirostris*). Arch. Virol. 133, 189–193. https://doi.org/10.1007/BF01309754.

Philippa, J.D.W., Leighton, F.A., Daoust, P.Y., Nielsen, O., Pagliarulo, M., Schwantje, H., Shury, T., Van Herwijen, R., Martina, B.E., Kuiken, T., Van de Bildt, M.W., Osterhaus, A.D., 2004. Antibodies to selected pathogens in free-ranging terrestrial carnivores and marine mammals in Canada. Vet. Rec. 155, 135–140. https://doi.org/10.7589/2013-07-155.

Reeves, R.R., Notarbartolo Di Sciara, G., 2006. The Status and Distribution of Cetaceans in the Black Sea and Mediterranean Sea. IUCN Centre for Mediterranean Cooperation, Malaga, Spain 137 pp.

Rice, D.W., 1998. Marine Mammals of the World: Systematics and Distribution. Society for Marine Mammalogy, Lawrence, Kansas, pp. 123–124.

Siegers, J.Y., van de Bildt, M., van Elk, C.E., Schürch, A.C., Tordo, N., Kuiken, T., Bodewes, R., Osterhaus, A., 2014. Genetic relatedness of dolphin rhabdovirus with rish rhabdoviruses. Emerg. Infect. Dis. 20, 1081–1082. https://doi.org/10.3201/eid2006.131880.

Tong, S., Chern, S.W., Li, Y., Pallansch, M.A., Anderson, L.J., 2008. Sensitive and broadly reactive reverse transcription-PCR assays to detect novel paramyxoviruses. J. Clin. Microbiol. Infect. 46, 2652–2658.

Tuomi, P.A., Murray, M.J., Garner, M.M., Goertz, C.E., Nordhausen, R.W., Burek-Huntington, K.A., Getzy, D.M., Nielsen, O., Archer, L.L., Maness, H.T., Waltzek, T.B., 2014. Novel poxvirus infection in northern and southern sea otters (*Enhydra lutris kenyoni* and *Enhydra lutris neiris*), Alaska and California. USA. J. Wildl. Dis. 50, 607–615. https://doi.org/10.7589/2013-08-217.

Van Beurden, S.J.I., Jsseldijk, L.L., van de Bildt, M.W.G., Begeman, L., Wellehan Jr., J.F.X., Waltzek, T.B., de Vrieze, G., Gröne, A., Kuiken, T., Verheije, M.H., Penzes, J.J., 2017. A novel cetacean adenovirus in stranded harbour porpoises from the North Sea: detection and molecular characterization. Arch. Virol. 162, 10.

Van Bressem, M.F., Kastelein, P.F., Orth, G., 1999a. Cutaneous papillomavirus infection in a harbour porpoise (*Phocoena phocoena*) from the North Sea. Vet. Rec. 144, 592–593.

Van Bressem, M.F., Van Waerebeek, K., Raga, J.A., 1999b. A review of virus infections of cetaceans and the potential impact of morbilliviruses, poxviruses and papillomaviruses on host population dynamics. Dis. Aquat. Org. 38, 53–65.

Van Elk, C., van de Bildt, M., van Run, P., de Jong, A., Getu, S., Verjans, G., Osterhaus, A., Kuiken, T., 2016. Central nervous system disease and genital disease in harbor porpoises (*Phocoena phocoena*) are associated with different herpesviruses. Vet. Res. 47, 28. https://doi.org/10.1186/s13567-016-0310-8.

VanDeVanter, D.R., Warrener, P., Bennett, L., Schultz, E.R., Coulter, S., Garber, R.L., Rose, T.M., 1996. Detection and analysis of diverse herpesviral species by consensus primer PCR. J. Clin. Microbiol. 34, 1666–1667.

Walker, P.J., Blasdell, K.R., Calisher, C.H., Dietzgen, R.G., Kondo, H., Kurath, G., Longdon, B., Stone, D.M., Tesh, R.B., Tordo, N., Vasilakis, N., Whitfield, A.E., 2018. ICTV report consortium. ICTV virus taxonomy profile: *rhabdoviridae*. J. Gen. Virol. 99, 447–448. https://doi.org/10.1099/jgv.0.001020.

Walker, P.J., Firth, C., Widen, S.G., Blasdell, K.R., Guzman, H., Wood, T.G., Paradkar, P.N., Holmes, E.C., Tesh, R.B., Vasilakis, N., 2015. Evolution of genome size and complexity in the Rhabdoviridae. PLoS Pathog. 11, e1004664. https://doi.org/10.1371/journal.ppat.1004664.

Wünschmann, A., Siebert, U., Weiss, R., 1999. Rhizopusmycosis in a harbour porpoise from the Baltic Sea. J. Wildl. Dis. 35, 569–573. https://doi.org/10.7589/0090-3558-35.3.569.